Prediction of miRNA-mRNA network regulating the migration ability of cytarabine-resistant HL60 cells

WAN-YI HSU[1-3], SHYH-SHIN CHIOU[1-4], PEI-CHIN LIN[1-4], YU-MEI LIAO[1-3], CHUNG-YU YEH[1] and YU-HSIN TSENG[1]

[1]Department of Pediatrics; [2]Division of Hematology and Oncology, Department of Pediatrics; [3]Special Hematologic Disease Service Center, Kaohsiung Medical University Hospital, Kaohsiung Medical University, Kaohsiung 80756; [4]Department of Pediatrics, School of Medicine, College of Medicine, Kaohsiung Medical University, Kaohsiung 80708, Taiwan, R.O.C.

Received August 16, 2023; Accepted December 1, 2023

DOI: 10.3892/br.2023.1708

Abstract. Cytarabine is an important medicine for acute myeloid leukemia (AML) treatment, however, drug resistance hinders the treatment of AML. Although microRNA (miRNA or miR) alteration is one of the well-recognized mechanisms underlying drug resistance in AML, few studies have investigated the role and function of miRNAs in the development of cytarabine resistance. In the present study, total RNA was isolated from parental HL60 and cytarabine-resistant HL60 (R-HL60) cells. Subsequently, miRNAs and mRNAs were detected using small RNA sequencing and gene expression array, respectively. Differentially expressed mRNAs (DEMs) and differentially expressed genes (DEGs) with more than two-fold changes between HL60 and R-HL60 cells were screened out. Negatively associated miRNA-mRNA pairs were selected as candidate miRNA-mRNA target pairs according to the miRDB, Targetscan or miRTar databases. Functional enrichment analysis of DEGs included in the candidate miRNA-mRNA pairs was performed. The results indicated that 10 DEGs (*CCL2*, *SOX9*, *SLC8A1*, *ICAM1*, *CXCL10*, *SIPR2*, *FGFR1*, *OVOL2*, *MITF* and *CARD10)* were simultaneously involved in seven Gene Ontology pathways related to the regulation of migration ability, namely the 'regulation of cell migration', 'regulation of locomotion', 'regulation of cellular component movement', 'cell migration', 'locomotion', 'cell motility', and 'localization of cell'. DEMs predicted to negatively regulate the aforementioned 10 DEGs were paired with DEGs into 16 candidate miRNA-mRNA pairs related to the regulation of migration ability. In addition, migration assays revealed that the migration ability of R-HL60 cells was greater than that of HL60 cells. These findings provide a new perspective for the treatment of cytarabine-resistant AML and advance our understanding of altered migration ability underlying cytarabine resistance development, specifically related to miRNAs.

Correspondence to: Dr Yu-Hsin Tseng, Department of Pediatrics, Kaohsiung Medical University Hospital, Kaohsiung Medical University, 100 Tzyou 1st Road, Kaohsiung 80756, Taiwan, R.O.C.
E-mail: 1040809@gap.kmu.edu.tw

Key words: acute myeloid leukemia, cytarabine resistance, HL60, microRNA, migration

Introduction

Acute myeloid leukemia (AML) cells arise from hematopoietic stem cells (HSCs) or myeloid progenitors in which key driver mutations have occurred (1). A subpopulation of leukemic cells within the malignant population, known as leukemia stem cells (LSCs), is considered to have self-renewing stem cell properties and are capable of initiating disease when engrafted into an immunocompromised host (2). The standard therapeutic approach for AML is cytarabine-based therapy that starts with induction chemotherapy [continuous infusion of cytarabine for 7 days concurrent with short infusions of anthracycline on each of the first 3 days (7+3 regimen)], followed by several cycles of consolidation chemotherapy or allogeneic HSC transplantation (3,4). However, only ~70% of patients receiving standard induction therapy achieve complete remission, and only 40% become long-term survivors (3,5). Older patients with AML exhibit stronger intrinsic resistance and less tolerance to chemotherapy than younger patients, resulting in a poor response to standard induction therapy (6). Intensive therapy with high-dose cytarabine improves the overall survival rate and reduces AML recurrence; however, the risk of drug-related side effects is also increased. AML treatment in older patients has not improved significantly in recent decades compared with that in younger patients (7). A more thorough understanding of the drug resistance mechanisms is required to provide effective cancer treatments and improve outcomes.

Cytarabine is a pyrimidine analog and converts into the triphosphate form within the cell. Cytarabine then incorporates into DNA strands during the S phase of the cell cycle to inhibit DNA synthesis (8). Insufficient cellular uptake and retention of cytarabine, overexpression of enzymes

that inactivate cytarabine, increased cellular deoxycytidine triphosphate (dCTP) pool, and increased DNA repair are the main mechanisms of cytarabine resistance (7). Overall, the reduced expression of human equilibrating nucleoside transporter 1 (hENT1) and deoxycytidine kinase (dCK) play pivotal roles during the development of cytarabine resistance in leukemia cells (7). However, other new mechanisms associated with cytarabine resistance have been discovered consecutively. In 2017, Farge *et al* reported that AML cells have increased oxidative phosphorylation after cytarabine treatment, and inhibition of oxidative phosphorylation could restore sensitivity to cytarabine (9). High-dose cytarabine-based therapy causes a decrease of the cytidine diphosphate pool that may accelerate the reduction of dCTP, thereby obstructing DNA synthesis. In addition, high-dose cytarabine treatment increases the AMP/ATP ratio that can trigger AMP-activated protein kinase and subsequently forkhead box class O, thereby promoting cell cycle arrest (10). However, therapeutic strategies to overcome cytarabine resistance have not been developed. A comprehensive understanding of the mechanisms underlying cytarabine resistance is necessary to optimize cytarabine therapy.

MicroRNAs (miRNAs or miRs) are highly-conserved single-stranded noncoding RNAs of ~22 nucleotides (11). In most cases, miRNAs induce mRNA degradation and translational repression by complementary binding to the 3'-untranslated region of the target mRNA (12). Although miRNAs do not participate in transcription and translation, they modify and control processes including cell division, self-renewal, invasion and DNA damage (13). MiRNA expression is known to be dysregulated in human cancers (14,15). Dysregulated miRNA expression by several mechanisms, such as copy number alterations, epigenetic changes, location of miRNA near oncogenomic regions and aberrant targeting of miRNA promoter regions, contribute AML pathogenesis (16). However, chemotherapy for AML often involves a combination of drugs that complicates research; thus, the role of miRNAs in drug resistance has not been thoroughly investigated. The role of miRNAs in leukemogenesis is unquestionable and miRNAs may prove to be an important addition to treatment of drug-resistant cancers in the future (17). Before specific miRNAs can be integrated into modern cancer therapies, clearly elucidating their mechanisms is necessary.

The present study provided comprehensive findings on differentially expressed miRNAs (DEMs) and differentially expressed genes (DEGs) during the development of cytarabine resistance in HL60 cells, revealing new opportunities for refractory or cytarabine-resistant AML.

Materials and methods

Cell culture. The R-HL60 cell line was established through the continuous treatment of parental HL60 cells (ATCC) with increasing concentrations of cytarabine as previously described (4). Both HL60 and R-HL60 cells were maintained in RPMI-1640 medium (Cytiva) containing 10% fetal bovine serum and 1% antibiotic-antimycotic solution (both from Gibco; Thermo Fisher Scientific, Inc.) under a humidified atmosphere of 5% CO_2 at 37˚C.

RNA isolation. Total RNA from HL60 and R-HL60 cells was extracted using TRIzol Reagent (Thermo Fisher Scientific, Inc.) according to the manufacturer's instructions. The RNA samples were submitted to Welgene Biotech. Co., Ltd. for small RNA sequencing and gene expression array analysis. RNA quantity was determined using an ND-1000 spectrophotometer (NanoDrop Technologies; Thermo Fisher Scientific, Inc.) and RNA quality was verified using an Agilent 2100 Bioanalyzer (Agilent Technologies, Inc.).

Small RNA sequencing. MiRNA sequencing libraries were prepared using the QIAseq miRNA Library Kit (cat. no. 331502; Qiagen GmbH) according to the manufacturer's protocol, and were sequenced using the NextSeq 500/550 High Output Kit (75 cycles; cat. no. FC-404-2005; Illumina, Inc.). The loading concentration of the final library was 1.6 pM, measured by High Sensitivity D1000 ScreenTape assay (High Sensitivity D1000 ScreenTape, cat. no. 5067-5584; and High Sensitivity D1000 Reagents, cat. no. 5067-5585; Agilent Technologies, Inc.). The type of sequencing setup was 75-bp single end. Sequencing data was processed using the Illumina software program BCL2FASTQ v2.20.0.422 (https://support.illumina.com/sequencing/sequencing_software/bcl2fastq-conversion-software/downloads.html). Subsequently, the Trimmomatic v0.36 program (http://www.usadellab.org/cms/?page=trimmomatic) was implemented to filter poor quality reads and trim poor quality bases on the basis of the quality score. Qualified reads after filtering low-quality data were analyzed using miRDeep2 v0.05 software (https://github.com/rajewsky-lab/mirdeep2) and were aligned to the reference genome downloaded from the University of California Santa Cruz (UCSC) Genome Browser (https://hgdownload.soe.ucsc.edu/downloads.html). miRNAs were mapped to few genomic locations; therefore, only reads that mapped perfectly to the genome with a ≤5-fold difference were used for miRNA identification.

Gene expression array. A Low Input Quick Amp Labeling Kit (cat. no. 5190-2305; Agilent Technologies, Inc.) was used to amplify 200 ng of total RNA and fluorescent Cy3 dye (included in the labeling kit; Agilent Technologies, Inc.) was used to label RNA oligonucleotides. A total of 600 ng Cy3-labeled cRNA was fragmented to an average size of 50-100 nucleotides by incubation with fragmentation buffer at 60˚C for 30 min. Correspondingly fragmented labeled cRNAs were pooled and hybridized to the SurePrint Microarray (Agilent Technologies, Inc.) at 65˚C for 17 h. The Cy3 microarray was scanned at 535 nm with an Agilent microarray scanner, and the scans were analyzed using Feature Extraction 10.7.3.1 software (Agilent Technologies, Inc.).

MiRNA-mRNA network analysis. The DEGs and DEMs with a fold change of ≥2 during the development of cytarabine resistance in HL60 cells were selected. The miRNA target genes were predicted using three online databases: miRDB, TargetScan, and miRTarBase (18-20). The miRNA-mRNA pairs with negative correlation were screened out on the basis of the hypothesis that miRNA negatively regulates the target mRNA. The miRNA-mRNA network was constructed by using Cytoscape 3.8.2 software (21).

Table I. Candidate miRNA-mRNA target pairs.

Small RNA sequencing			Gene expression array
miRNA	Fold change	Up/Down	mRNA (fold change)
hsa-miR-1-3p	-5.74	Down	*SLC8A1* (3.06), *CCL2* (2.52), *SOX9* (3.30), *AIM2* (7.67)
hsa-miR-1255b-5p	-2.34		*GAS7* (2.15), *ICAM1* (5.83), *CPS1* (2.03)
hsa-miR-1285-3p	-2.57		*S1PR2* (2.68), *CXCL10* (74.65)
hsa-miR-155-5p	-152.00		*CCL2* (2.52), *ICAM1* (5.83)
hsa-miR-200c-5p	-3.51		*PSMB9* (2.28), *CXCL10* (74.65)
hsa-miR-224-5p	-7.62		*PTX3* (2.75)
hsa-miR-3168	-109.00		*TAGLN3* (2.30)
hsa-miR-34a-5p	-2.05		*CYBB* (4.76), *SPTBN1* (2.45), *CD70* (11.63), *BIRC3* (17.74)
hsa-miR-3609	-3.51		*CXCL10* (74.65), *CPS1* (2.03), *PMAIP1* (2.06)
hsa-miR-548ag	-2.35		*PMAIP1* (2.06)
hsa-miR-548q	-5.23		*IL10RA* (2.26)
hsa-miR-96-3p	-2.45		*ARL4C* (2.26)
hsa-miR-124-3p	6.32	Up	*MITF* (-14.97), *REEP1* (-2.49), *OVOL2* (-2.39), *SMPDL3A* (-2.18), *FGFR1* (-11.23), *PTPN14* (-2.58)
hsa-miR-1290	2.03		*IKZF2* (-12.80)
hsa-miR-146a-5p	90.38		*CARD10* (-3.37)
hsa-miR-3150a-3p	3.02		*PTPN14* (-2.58), *CARD10* (-3.37)
hsa-miR-497-5p	2.18		*C1orf226* (-2.08), *CARD10* (-3.37)

miRNA or miR, microRNA; Up, upregulated; Down, downregulated.

Functional enrichment analysis. Gene ontology (GO) analysis was performed using ShinyGO 0.76 to determine the biological functions of the DEGs included in the candidate miRNA-mRNA network (22,23). Protein-protein interaction analysis in the cluster associated with the regulation of cell migration, locomotion, cellular component movement, cell motility, and localization was performed using STRING 11.5 (24).

Transwell migration assay. A Transwell chamber consisting of an upper and a lower chamber separated by a porous membrane was used for the cell migration assay. Cells were suspended in serum-free RPMI-1640 medium and plated in the upper chamber with 8-μm pores (Guangzhou Jet Biofiltration Co., Ltd.), adjusting the cell concentration to 2.5x10^5 cells/ml. RPMI-1640 medium with 10% fetal bovine serum was added to the lower chamber. The Transwell chamber was incubated in an incubator with 5% CO_2 at 37˚C, and then the cells in the lower chamber were collected and counted by Cell Counting Kit-8 (CCK-8) assay (Energenesis Biomedical Co., Ltd.) after incubating for 24 and 48 h. In detail, a 200-μl volume obtained from the lower chamber was transferred to a 96-well plate, then 20 μl CCK-8 solution was added per well and incubation followed for 2 h. Subsequently, the specific absorbance and reference absorbance of each well were measured at 450 and 650 nm, respectively, by an enzyme-linked immunosorbent assay reader (Epoch2; Agilent Technologies, Inc.).

Statistical analysis. Data were analyzed using GraphPad Prism 5.0 (GraphPad Software Inc.; Dotmatics). A Student's paired t-test was used to determine the differences between the experimental and control groups. Data are representative of three independent experiments, with values presented as the mean ± standard deviation and $P<0.05$ was considered to indicate a statistically significant difference.

Results

DEGs and DEMs between HL60 and R-HL60 cells. To investigate the alterations of miRNA and mRNA profiles during the development of cytarabine resistance in HL60 cells, miRNA and mRNA profiles of HL60 and R-HL60 cells were determined using small RNA sequencing and gene expression array analysis, respectively. The flowchart of candidate miRNA-mRNA target pair selections and subsequent functional enrichment analysis is displayed in Fig. 1. The standard setting for identifying DEMs was >1 read per million (RPM). DEMs and DEGs, with an adjusted P-value <0.05 were considered statistically significant and selected for further investigation. In the present study, the experimental design of previous studies was referred to and DEMs and DEGs whose expression changes between HL60 and R-HL60 cells were ≥2-fold were selected for analysis (25,26). Small RNA sequencing data revealed that there were 75 DEMs with a ≥2-fold difference between HL60 and R-HL60 cells, of which 34 DEMs had higher expression levels in R-HL60 than those in parental HL60 cells, and 41 DEMs had lower expression levels in R-HL60 than those in parental HL60 cells. Gene expression array data showed that there were 274 DEGs

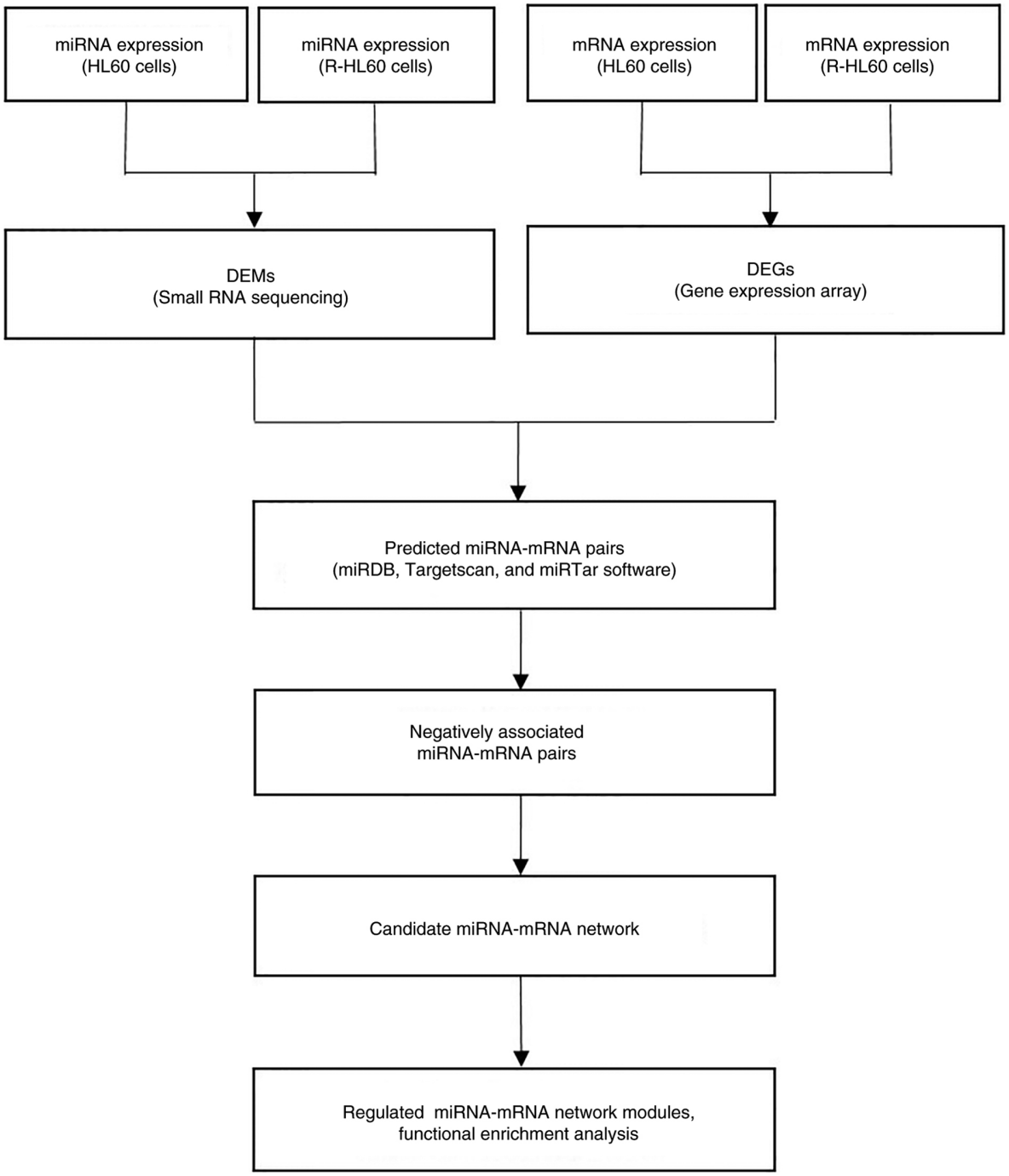

Figure 1. Flowchart of candidate miRNA-mRNA target pair selection. Expression profiles of miRNA and mRNA in HL60 and R-HL60 cells were detected using small RNA sequencing and gene expression array, respectively. Expression of miRNAs and mRNAs with a ≥2-fold difference between HL60 and R-HL60 cells were selected. Putative target gene sets of DEMs were predicted using three databases (miRDB, Targetscan, and miRTar). A miRNA-mRNA network with negative associations was integrated and functional (GO) analysis was performed. miRNA, microRNA; DEMs, differentially expressed mRNAs; GO, Gene Ontology; DEGs, differentially expressed genes.

with a ≥2-fold difference between R-HL60 and HL60 cells, of which 185 DEGs had higher expression levels in R-HL60 than those in parental HL60 cells, and 89 DEGs had lower expression levels in R-HL60 than those in parental HL60 cells. Negatively associated miRNA-mRNA pairs predicted using the miRDB, Targetscan, or miRTar database were selected as candidate miRNA-mRNA target pairs. Candidate miRNA-mRNA target pairs including 17 DEMs (5 upregulated miRNAs and 12 downregulated miRNAs) and 28 DEGs (19 upregulated genes and 9 downregulated genes) are presented in Table I. Heat maps revealing the hierarchical clustering of 17 DEMs and 28 DEGs are shown in Fig. 2, and the candidate miRNA-mRNA network was visualized using Cytoscape 3.8.2 software (Fig. 3).

Functional enrichment analysis of DEGs. Functional enrichment analysis was performed for 28 DEGs included in the candidate miRNA-mRNA target pairs. The histogram

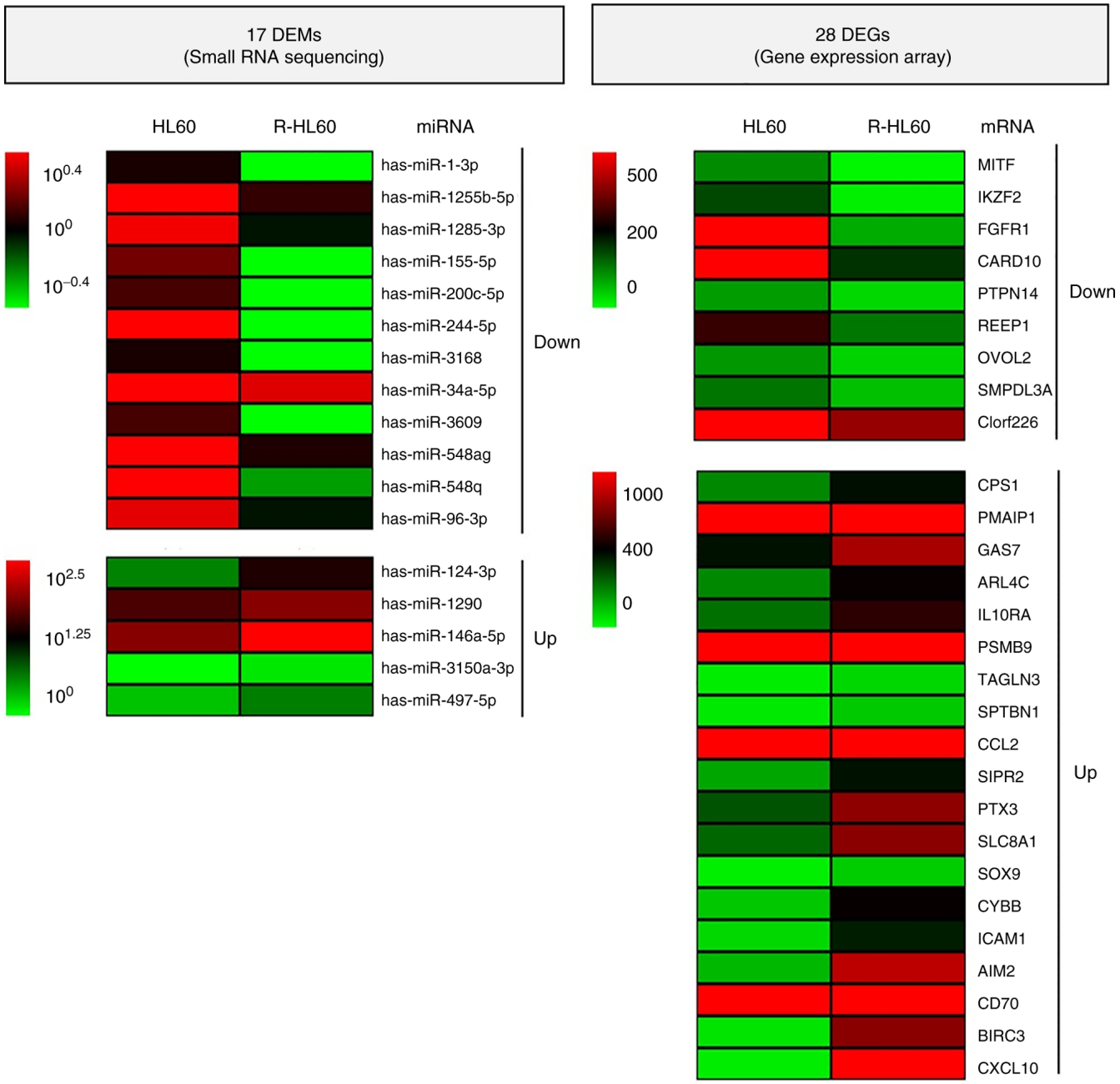

Figure 2. Heatmaps of DEMs and DEGs. The hierarchical clustering of 17 DEMs (left) and 28 DEGs (right) included in candidate miRNA-mRNA target pairs was performed. Upregulated and downregulated genes are colored in red and green, respectively. DEMs, differentially expressed mRNAs; DEGs, differentially expressed genes; miR, microRNA.

of the top 20 most-enriched GO pathways is displayed in Fig. 4A, and genes involved in the GO pathways are listed in Table II. The hierarchical clustering tree revealed the relationships between similar sets of data (Fig. 4B). In addition, 10 gene*s (CCL2, SOX9, SLC8A1, ICAM1, CXCL10, SIPR2, FGFR1, OVOL2, MITF and CARD10) w*ere simultaneously involved in seven GO terms related to the regulation of migration ability, namely 'regulation of cell migration', 'regulation of locomotion', 'regulation of cellular component movement', 'cell migration', 'locomotion', 'cell motility', and 'localization of cell'. The modulation of migration ability is considered as a possible therapeutic target in refractory AML (27), therefore, the present study focused on analyzing the candidate miRNA-mRNA pairs associated with the modulation of migration ability. The candidate miRNA-mRNA pairs involved in these GO terms associated with the regulation of migration ability are listed in Table III. Among them, SIPR2 was not present in the STRING database; therefore, protein-protein interaction analysis was performed for the remaining nine genes in the cluster (Fig. 4C). In addition, the interactive graph displays the percentage of shared gene members for the enriched GO terms (Fig. 4D).

Comparison of migration ability between HL60 and R-HL60. Transwell migration assays were used to compare the migration

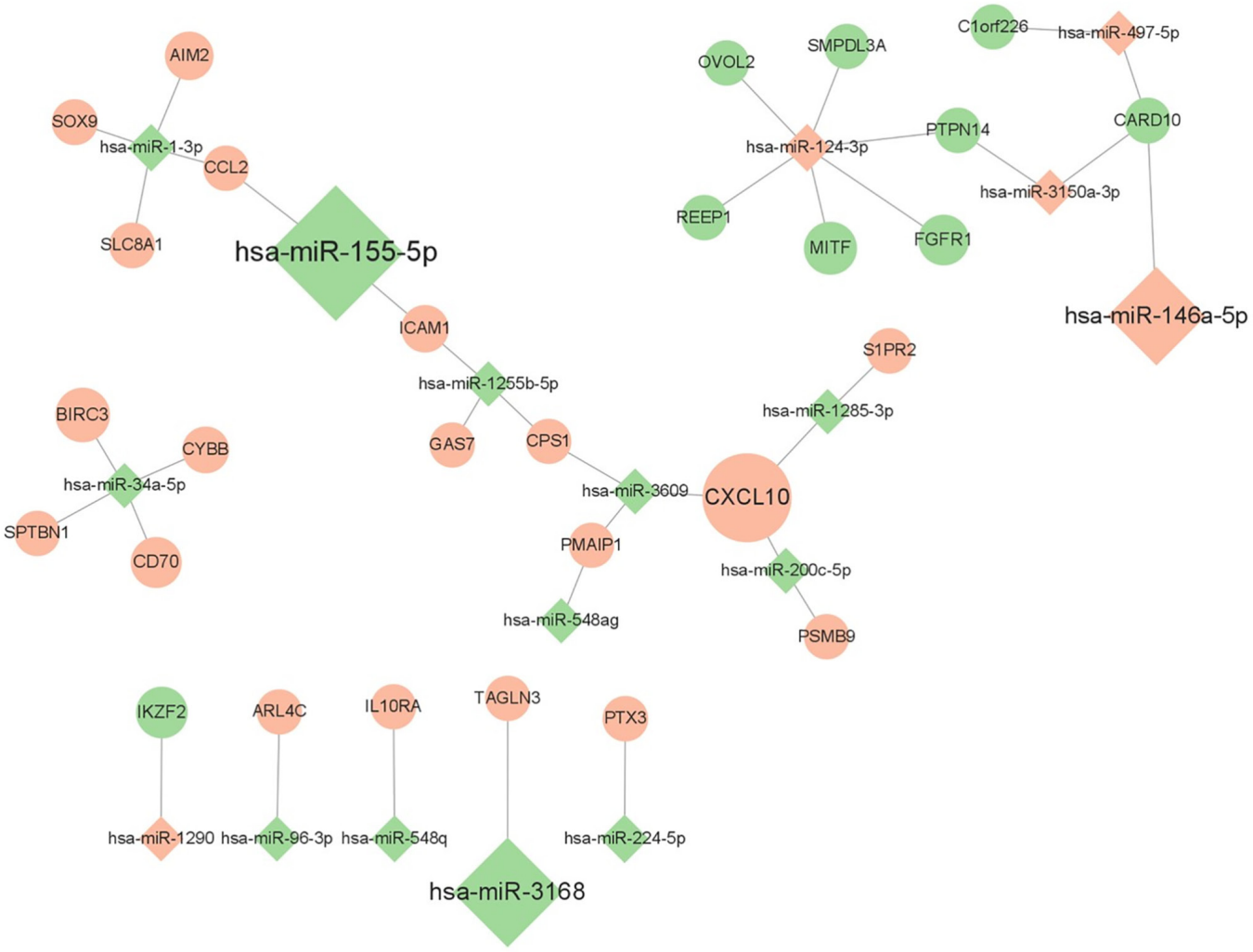

Figure 3. MiRNA-mRNA network. Candidate miRNA-mRNA target pairs including 17 differentially expressed mRNAs and 28 differentially expressed genes were integrated in the network. Circles and diamonds represent mRNA and miRNAs, respectively. Upregulated and downregulated genes are colored in orange and green, respectively. The size of the pattern represents the fold change in expression between HL60 and R-HL60 cells. miRNA, microRNA.

ability of HL60 and R-HL60 cells. The results showed that the migration ability of R-HL60 cells was ~2-folds higher than that of parental HL60 cells following incubation for 24 h, and was ~3-folds higher than that of parental HL60 cells following incubation for 48 h (Fig. 5).

Discussion

Cytarabine is the main drug used for AML treatment, however, drug resistance hinders the achievement of complete remission. Although miRNAs are known to be often dysregulated in AML, the role of miRNAs in the development of drug resistance has not been thoroughly investigated. The present study, to the best of the authors' knowledge, is the first to comprehensively compare the integrated miRNA-mRNA network between HL60 and R-HL60 cells, and reveal that 16 miRNA-mRNA pairs, including miR-1-3p/*CCL2*, miR-1-3p/*SOX9*, miR-1-3p/*SLC8A1*, miR-155-5p/*CCL2*, miR-155-5p/*ICAM1*, miR-1255b-5p/*ICAM1*, miR-200c-5p/*CXCL10*, miR-3609/*CXCL10*, miR-1285-3p/*SIPR2*, miR-1285-3p/*CXCL10*, miR-124-3p/*FGFR1*, miR-124-3p/*OVOL2*, miR-124-3p/*MITF*, miR-146a-5p/*CARD10*, miR-497a-5p/*CARD10*, and miR-3150a-3p/*CARD10*, participate in the regulation of migration ability during the development of cytarabine resistance in HL60 cells (Table III). Among them, miR-1-3p targeting *CCL2* (28); miR-1-3p targeting *SOX9* (29); miR-1-3p targeting *SLC8A1* (30); and miR-146-5p targeting *CARD10* (31) have been confirmed by luciferase assay in previous studies. In addition, miR-1-3p (32), miR-1255-5p (33), miR-200c-5p (34), miR-155-5p (35), miR-1285-3p (36), miR-124-3p (37) and miR-146a-5p (38,39) have been also reported to regulate cell migratory behavior in several cell models.

Several studies have reported associations between miRNAs and AML outcomes. For example, patients with high expression levels of miR-126-5p/3p had poor survival. Transfection of the mimic miR-126-5p into an AML cell line (KG-1) resulted in decreased sensitivity to cytarabine (40). A specific anti-miR-21 oligonucleotide (AMO-miR-21) inhibited cell viability and induced apoptosis in HL60 cells. AMO-miR-21 in combination with cytarabine enhanced the sensitivity to cytarabine and promoted cytarabine-induced

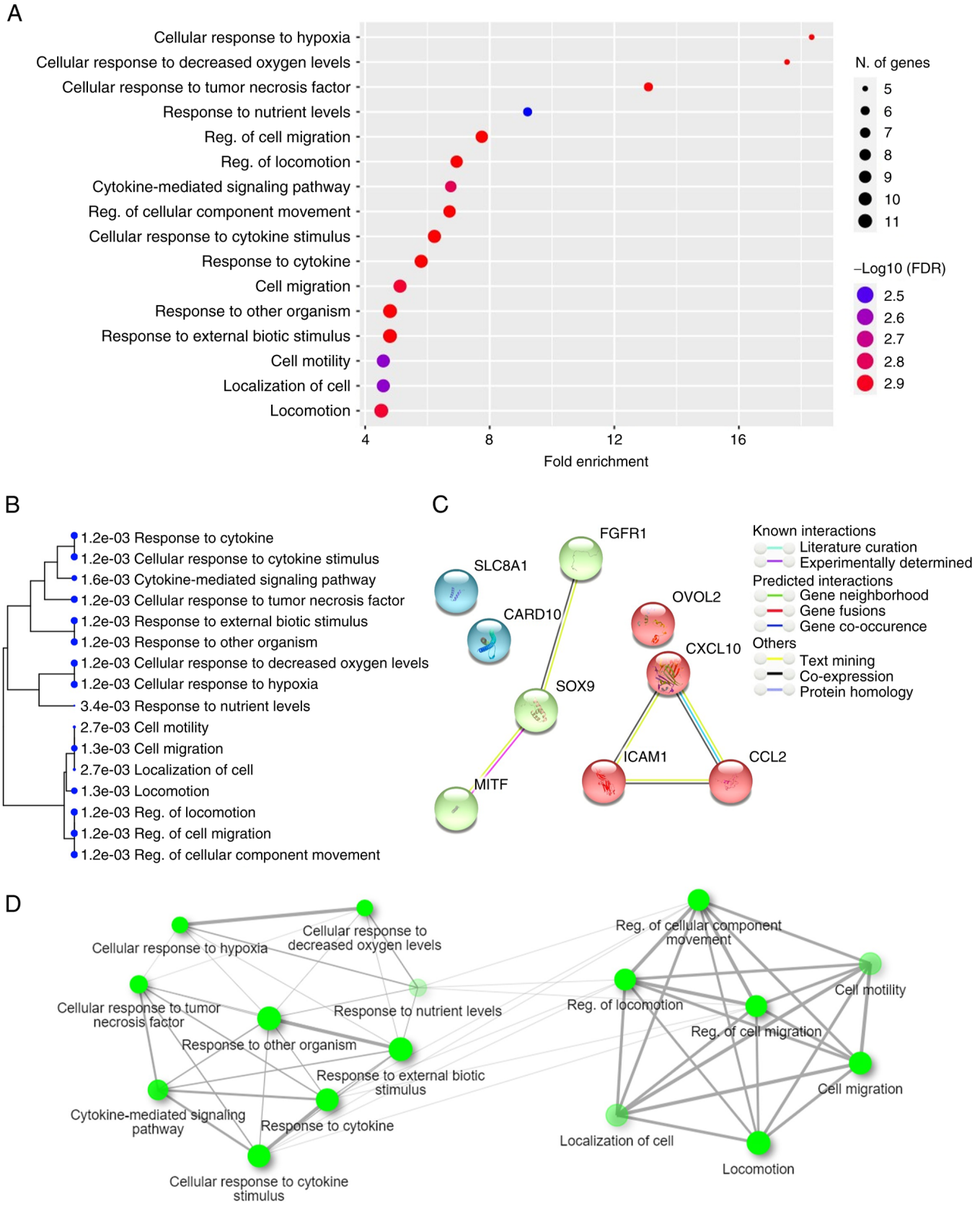

Figure 4. Functional enrichment of candidate DEGs. Genes involved in the candidate miRNA-mRNA network were considered as candidate targets and their functional enrichment was analyzed. (A) Histogram of the top 20 most-enriched GO terms of candidate DEGs. (B) A hierarchical clustering tree summarizes the association between significant GO terms. GO terms shared by a high percentage of gene members are clustered together. The size of the dots indicates the significance of the P-value. (C) Ten genes (*CCL2*, *SOX9*, *SLC8A1*, *ICAM1*, *CXCL10*, *SIPR2*, *FGFR1*, *OVOL2*, *MITF* and *CARD10*) were simultaneously involved in seven GO pathways, including regulation of 'cell migration', 'regulation of locomotion', 'regulation of cellular component movement', 'cell migration', 'locomotion', 'cell motility', and 'localization of cell'. A network cluster analysis of protein-protein interaction was performed using the STRING software. (D) An interactive graph revealed the association between enriched GO terms. Two terms (nodes) are connected if they share ≥20% of gene members. Darker nodes represent more significantly enriched gene terms. Larger nodes represent larger gene sets. Thicker edges represent more overlapped genes.

Table II. Top 20 most-enriched GO pathways involved in the development of cytarabine resistance in HL60 cells.

GO ID	Enrichment FDR	Fold enrichment	GO pathway	mRNA
GO:0071456	0.001178771	18.33655084	Cellular response to hypoxia	*ICAM1 PMAIP1 CYBB SLC8A1 PSMB9*
GO:0036294	0.001178771	17.54618227	Cellular response to decreased oxygen levels	*ICAM1 PMAIP1 CYBB SLC8A1 PSMB9*
GO:0071356	0.001178771	13.09613175	Cellular response to tumor necrosis factor	*BIRC3 ICAM1 CCL2 CD70 AIM2*
GO:0031667	0.003377186	9.21671159	Response to nutrient levels	*CPS1 ICAM1 PMAIP1 CYBB CXCL10 SLC8A1*
GO:0030334	0.001169267	7.745545153	Regulation of cell migration	*FGFR1 ICAM1 CARD10 CCL2 SOX9 CXCL10 SLC8A1 MITF S1PR2*
GO:0040012	0.001169267	6.938717532	Regulation of locomotion	*FGFR1 ICAM1 CARD10 CCL2 SOX9 CXCL10 SLC8A1 MITF S1PR2*
GO:0019221	0.001551712	6.749370836	Cytokine-mediated signaling pathway	*BIRC3 ICAM1 CCL2 IL10RA CD70 AIM2 CXCL10 PSMB9*
GO:0051270	0.001169267	6.709968603	Regulation of cellular component movement	*FGFR1 ICAM1 CARD10 CCL2 SOX9 CXCL10 SLC8A1 MITF S1PR2*
GO:0071345	0.001169267	6.22433377	Cellular response to cytokine stimulus	*BIRC3 ICAM1 CCL2 IL10RA SOX9 CD70 PTPN14 AIM2 CXCL10 PSMB9*
GO:0034097	0.001169267	5.798738299	Response to cytokine	*BIRC3 ICAM1 CCL2 IL10RA SOX9 CD70 PTPN14 AIM2 CXCL10 PSMB9*
GO:0016477	0.00133677	5.120395328	Cell migration	*FGFR1 ICAM1 CARD10 CCL2 SOX9 OVOL2 CXCL10 SLC8A1 MITF S1PR2*
GO:0051707	0.001178771	4.799341602	Response to other organism	*CPS1 BIRC3 ICAM1 CCL2 IL10RA PMAIP1 AIM2 PTX3 CYBB CXCL10 PSMB9*
GO:0043207	0.001178771	4.796770985	Response to external biotic stimulus	*CPS1 BIRC3 ICAM1 CCL2 IL10RA PMAIP1 AIM2 PTX3 CYBB CXCL10 PSMB9*
GO:0048870	0.002712992	4.584137709	Cell motility	*FGFR1 ICAM1 CARD10 CCL2 SOX9 OVOL2 CXCL10 SLC8A1 MITF S1PR2*
GO:0051674	0.002712992	4.584137709	Localization of cell	*FGFR1 ICAM1 CARD10 CCL2 SOX9 OVOL2 CXCL10 SLC8A1 MITF S1PR2*
GO:0040011	0.00133677	4.51845178	Locomotion	*FGFR1 ICAM1 CARD10 CCL2 SPTBN1 SOX9 OVOL2 CXCL10 SLC8A1 MITF S1PR2*

GO, Gene Ontology; FDR, false discovery rate.

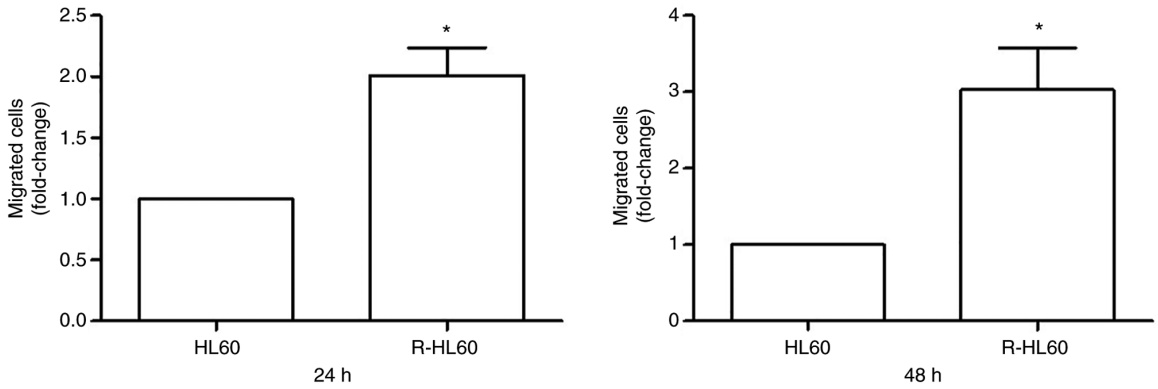

Figure 5. Comparison of the migration ability between HL60 and R-HL60 cells. HL60 and R-HL60 cells migrated to the lower chamber of a Transwell chamber after incubation for 24 and 48 h, and were then collected and counted using a CCK-8 assay. R-HL60 cells had a higher migration ability than parental HL60 cells. Data are presented as the mean ± standard deviation of three independent experiments. *P<0.05 indicated a statistically significant difference compared with HL60 cells.

Table III. Integration of miRNA-mRNA pairs involved in the regulation of cell migration behavior or ability during the development of cytarabine resistance in HL60 cells.

miRNA	Up/Down	mRNA	Up/Down	GO pathway
hsa-miR-1-3p	Down	*CCL2*, *SOX9*, *SLC8A1*	Up	• Regulation of cell migration
hsa-miR-155-5p		*CCL2*, *ICAM1*		• Regulation of locomotion
hsa-miR-1255b-5p		*ICAM1*		• Regulation of cellular component movement
hsa-miR-200c-5p		*CXCL10*		• Cell migration
hsa-miR-3609				• Locomotion
hsa-miR-1285-3p		*S1PR2*, *CXCL10*		• Cell motility
hsa-miR-124-3p	Up	*FGFR1*, *OVOL2*, *MITF*	Down	• Localization of cell
hsa-miR-146a-5p		*CARD10*		
hsa-miR-497a-5p				
hsa-miR-3150a-3p				

miRNA or miR, microRNA; GO, Gene Ontology; up, upregulated; down, downregulated.

apoptosis. These effects of AMO-miR-21 may be partially due to upregulated *PDCD4*, a direct target of miR-21 (41). In addition, miRNA-181a overexpressed in AML cells downregulated the expression of ataxia telangiectasia mutated (ATM), a DNA damage response protein. Thus, DNA damage could not be repaired by ATM, leading to uncontrolled growth and drug resistance in AML cells (42). However, it is considered that comparing drug-resistant cells with parental cells would reveal the actual mechanisms of drug resistance more effectively than studying chemotherapy sensitivity on parental cells alone.

Unlike solid cancers, which gradually acquire motility, leukemia has inherent cell motility ability as leukocytes that move throughout the vascular system. The precise location of leukemia origin is often unknown, which has led to controversy about whether leukemia should be considered a metastatic disease (1). Even so, widespread organotropic dissemination is a common feature of liquid and solid cancers. It was revealed that high-dose cytarabine treatment inhibited the migratory ability of the C1498 AML cell line and that of the MLL-AF9 oncogene-induced AML mouse model (27,43). However, proliferative C1498 cells could restore migratory ability after relapse (27). Although the association between migration ability and chemotherapy resistance is complex and not yet clarified, modulation of migration ability is considered as a possible therapeutic target in refractory AML (27).

The lack of validation in other drug-resistant cell lines and clinical specimens is a limitation of the present study. However, the study revealed the possible mechanisms underlying the regulation of cell migration ability during the development of cytarabine resistance in HL60 cells. This may assist in the development of targeted therapies for modulating cell migration in refractory AML.

Acknowledgements

Not applicable.

Funding

The present study was supported by the National Science and Technology Council of Taiwan (grant no. MOST 109-2314-B-037-103-MY3 and NSTC 112-2314-B-037-063) and the Kaohsiung Medical University Hospital (Kaohsiung, Taiwan) (grant nos. KMUH109-9R49, KMUH110-0R45 and KMUH111-1R42).

Availability of data and materials

The datasets used and/or analyzed during the current study are available from the corresponding author on reasonable request. The sequencing datasets generated and/or analyzed during the current study are available in the Gene Expression Omnibus repository (https://www.ncbi.nlm.nih.gov/geo/query/acc.cgi?acc=GSE221719).

Authors' contributions

WYH, SSC and YHT conceived and designed the experiments. PCL, YML and CYY performed the experiments and data analysis. CYY and YHT confirm the authenticity of all the raw data. WYH wrote the manuscript. YHT edited the manuscript. All authors read and approved the final manuscript.

Ethics approval and consent to participate

Not applicable.

Patient consent for publication

Not applicable.

Competing interests

The authors declare that they have no competing interests.

References

1. Whiteley AE, Price TT, Cantelli G and Sipkins DA: Leukaemia: A model metastatic disease. Nat Rev Cancer 21: 461-475, 2021.
2. Vetrie D, Helgason GV and Copland M: The leukaemia stem cell: Similarities, differences and clinical prospects in CML and AML. Nat Rev Cancer 20: 158-173, 2020.
3. Dombret H and Gardin C: An update of current treatments for adult acute myeloid leukemia. Blood 127: 53-61, 2016.
4. Tseng YH, Chiou SS, Weng JP and Lin PC: Curcumin and tetrahydrocurcumin induce cell death in Ara-C-resistant acute myeloid leukemia. Phytother Res 33: 1199-1207, 2019.
5. Tseng YH, Yang RC, Chiou SS, Shieh TM, Shih YH and Lin PC: Curcumin induces apoptosis by inhibiting BCAT1 expression and mTOR signaling in cytarabine-resistant myeloid leukemia cells. Mol Med Rep 24: 565, 2021.
6. Yanada M and Naoe T: Acute myeloid leukemia in older adults. Int J Hematol 96: 186-193, 2012.
7. Wang SY, Shih YH, Shieh TM and Tseng YH: Proteasome inhibitors interrupt the activation of Non-Canonical NF-κB signaling pathway and induce cell apoptosis in Cytarabine-Resistant HL60 cells. Int J Mol Sci 23: 361, 2021.
8. Bhise NS, Chauhan L, Shin M, Cao X, Pounds S, Lamba V and Lamba JK: MicroRNA-mRNA pairs associated with outcome in AML: From in vitro Cell-Based studies to AML patients. Front Pharmacol 6: 324, 2015.
9. Farge T, Saland E, de Toni F, Aroua N, Hosseini M, Perry R, Bosc C, Sugita M, Stuani L, Fraisse M, *et al*: Chemotherapy-Resistant human acute myeloid leukemia cells are not enriched for leukemic stem cells but require oxidative metabolism. Cancer Discov 7: 716-735, 2017.
10. Li Z, Guo JR, Chen QQ, Wang CY, Zhang WJ, Yao MC and Zhang W: Exploring the antitumor mechanism of high-dose cytarabine through the metabolic perturbations of ribonucleotide and deoxyribonucleotide in human promyelocytic Leukemia HL-60 Cells. Molecules 22: 499, 2017.
11. Yen MC, Yeh IJ, Liu KT, Jian SF, Lin CJ, Tsai MJ and Kuo PL: Next-generation sequencing predicts interaction network between miRNA and target genes in lipoteichoic acid-stimulated human neutrophils. Int J Mol Med 44: 1436-1446, 2019.
12. Liu Y, Cheng Z, Pang Y, Cui L, Qian T, Quan L, Zhao H, Shi J, Ke X and Fu L: Role of microRNAs, circRNAs and long noncoding RNAs in acute myeloid leukemia. J Hematol Oncol 12: 51, 2019.
13. Zhang J, Gu Y and Chen B: Mechanisms of drug resistance in acute myeloid leukemia. Onco Targets Ther 12: 1937-1945, 2019.
14. Yu DS, Song XL and Yan C: Oncogenic miRNA-1908 targets HDAC10 and promotes the aggressive phenotype of cervical cancer cell. Kaohsiung J Med Sci 37: 402-410, 2021.
15. Ali Syeda Z, Langden SSS, Munkhzul C, Lee M and Song SJ: Regulatory mechanism of MicroRNA expression in cancer. Int J Mol Sci 21: 1723, 2020.
16. Trino S, Lamorte D, Caivano A, Laurenzana I, Tagliaferri D, Falco G, Del Vecchio L, Musto P and De Luca L: MicroRNAs as new biomarkers for diagnosis and prognosis, and as potential therapeutic targets in acute myeloid leukemia. Int J Mol Sci 19: 460, 2018.
17. Gabra MM and Salmena L: microRNAs and acute myeloid leukemia chemoresistance: A mechanistic overview. Front Oncol 7: 255, 2017.
18. Chou CH, Shrestha S, Yang CD, Chang NW, Lin YL, Liao KW, Huang WC, Sun TH, Tu SJ, Lee WH, *et al*: miRTarBase update 2018: A resource for experimentally validated microRNA-target interactions. Nucleic Acids Res 46: D296-D302, 2018.
19. Liu W and Wang X: Prediction of functional microRNA targets by integrative modeling of microRNA binding and target expression data. Genome Biol 20: 18, 2019.
20. Garcia DM, Baek D, Shin C, Bell GW, Grimson A and Bartel DP: Weak seed-pairing stability and high target-site abundance decrease the proficiency of lsy-6 and other microRNAs. Natu Struct Mol Biol 18: 1139-1146, 2011.
21. Shannon P, Markiel A, Ozier O, Baliga NS, Wang JT, Ramage D, Amin N, Schwikowski B and Ideker T: Cytoscape: A software environment for integrated models of biomolecular interaction networks. Genome Res 13: 2498-2504, 2003.
22. Escandón M, Lamelas L, Roces V, Guerrero-Sanchez VM, Meijón M and Valledor L: Protein interaction Networks: Functional and statistical approaches. Methods Mol Biol 2139: 21-56, 2020.
23. Ge SX, Jung D and Yao R: ShinyGO: A graphical gene-set enrichment tool for animals and plants. Bioinformatics 36: 2628-2629, 2020.
24. Szklarczyk D, Gable AL, Lyon D, Junge A, Wyder S, Huerta-Cepas J, Simonovic M, Doncheva NT, Morris JH, Bork P, *et al*: STRING v11: Protein-protein association networks with increased coverage, supporting functional discovery in genome-wide experimental datasets. Nucleic Acids Res 47: D607-D613, 2019.
25. Guo J, Zhou X, Cheng L and Gao X: Construction of a miRNA-mRNA network related to exosomes in metastatic hepatocellular carcinoma. Heliyon 9: e15428, 2023.
26. Wei SY, Guo S, Feng B, Ning SW and Du XY: Identification of miRNA-mRNA network and immune-related gene signatures in IgA nephropathy by integrated bioinformatics analysis. BMC Nephrol 22: 392, 2021.
27. Morimatsu M, Yamashita E, Seno S, Sudo T, Kikuta J, Mizuno H, Okuzaki D, Motooka D and Ishii M: Migration arrest of chemoresistant leukemia cells mediated by MRTF-SRF pathway. Inflamm Regen 40: 15, 2020.
28. Li P, Li Y, Dai Y, Wang B, Li L, Jiang B, Wu P and Xu J: The LncRNA H19/miR-1-3p/CCL2 axis modulates lipopolysaccharide (LPS) stimulation-induced normal human astrocyte proliferation and activation. Cytokine 131: 155106, 2020.
29. Zhang H, Zhang Z, Gao L, Qiao Z, Yu M, Yu B and Yang T: miR-1-3p suppresses proliferation of hepatocellular carcinoma through targeting SOX9. Onco Targets Ther 12: 2149-2157, 2019.
30. Yang Y, Yang H, Lian X, Yang S, Shen H, Wu S, Wang X and Lyu G: Circulating microRNA: Myocardium-derived prenatal biomarker of ventricular septal defects. Front Genet 13: 899034, 2022.
31. Cowan C, Muraleedharan CK, O'Donnell JJ III, Singh PK, Lum H, Kumar A and Xu S: MicroRNA-146 inhibits thrombin-induced NF-κB activation and subsequent inflammatory responses in human retinal endothelial cells. Invest Ophthalmol Vis Sci 55: 4944-4951, 2014.
32. Xu M, Sun J, Yu Y, Pang Q, Lin X, Barakat M, Lei R and Xu J: TM4SF1 involves in miR-1-3p/miR-214-5p-mediated inhibition of the migration and proliferation in keloid by regulating AKT/ERK signaling. Life Sci 254: 117746, 2020.
33. Zhao Y, Tang X, Zhao Y, Yu Y and Liu S: Diagnostic significance of microRNA-1255b-5p in prostate cancer patients and its effect on cancer cell function. Bioengineered 12: 11451-11460, 2021.
34. Li Y, Bai W and Zhang J: MiR-200c-5p suppresses proliferation and metastasis of human hepatocellular carcinoma (HCC) via suppressing MAD2L1. Biomed Pharmacother 92: 1038-1044, 2017.
35. Al-Haidari A, Algaber A, Madhi R, Syk I and Thorlacius H: MiR-155-5p controls colon cancer cell migration via post-transcriptional regulation of Human Antigen R (HuR). Cancer Lett 421: 145-151, 2018.
36. Zhang Y and Ruan F: LncRNA LEF1-AS1 promotes ovarian cancer development through interacting with miR-1285-3p. Cancer Manag Res 12: 687-694, 2020.
37. Wu Q, Zhong H, Jiao L, Wen Y, Zhou Y, Zhou J, Lu X, Song X and Ying B: MiR-124-3p inhibits the migration and invasion of Gastric cancer by targeting ITGB3. Pathol Res Pract 216: 152762, 2020.
38. Sathyanarayanan A, Chandrasekaran KS and Karunagaran D: microRNA-146a inhibits proliferation, migration and invasion of human cervical and colorectal cancer cells. Biochem Biophys Res Commun 480: 528-533, 2016.
39. Liu Q, Wang W, Yang X, Zhao D, Li F and Wang H: MicroRNA-146a inhibits cell migration and invasion by targeting RhoA in breast cancer. Oncol Rep 36: 189-196, 2016.
40. Shibayama Y, Kondo T, Ohya H, Fujisawa S, Teshima T and Iseki K: Upregulation of microRNA-126-5p is associated with drug resistance to cytarabine and poor prognosis in AML patients. Oncol Rep 33: 2176-2182, 2015.
41. Li Y, Zhu X, Gu J, Hu H, Dong D, Yao J, Lin C and Fei J: Anti-miR-21 oligonucleotide enhances chemosensitivity of leukemic HL60 cells to arabinosylcytosine by inducing apoptosis. Hematology 15: 215-221, 2010.
42. Liu X, Liao W, Peng H, Luo X, Luo Z, Jiang H and Xu L: miR-181a promotes G1/S transition and cell proliferation in pediatric acute myeloid leukemia by targeting ATM. J Cancer Res Clin Oncol 142: 77-87, 2016.
43. Duarte D, Amarteifio S, Ang H, Kong IY, Ruivo N, Pruessner G, Hawkins ED and Lo Celso C: Defining the in vivo characteristics of acute myeloid leukemia cells behavior by intravital imaging. Immunol Cell Biol 97: 229-235, 2019.